International Journal of Enhanced Research in Science, Technology & Engineering
ISSN: 2319-7463, Vol. 5 Issue 7, July-2016

Fully-printed organic PTAT voltage generators designed using a fast technique modeling

M.A.Sankhare[1], E. Bergeret[2], P. Pannier[3], R. Coppard[4]

[1,2,3] IM2NP (UMR 7334), Campus de Saint-Jérôme, Avenue Escadrille Normandie Niémen - Case 142, F-13397, France
[4]Laboratoire des Composants Imprimés, LITEN-LCEI, CEA-Grenoble, France

ABSTRACT

In this paper, the simulations and measurements of the first organic Proportional To Absolute Temperature (PTAT) voltage generators are presented. The circuits are based on fully-printed top-gate bottom-contact Organic Thin Film Transistors (OTFTs). The transistors, realized on a PEN (Polyethylene Naphtalate) flexible substrate respectively use Polytriarylamine and Acene-based diimide as organic semiconductors for P-type and N-Type. An iterative extraction procedure published in our previous work is applied to OTFTs with W/L ratios between 25 and 400 at temperatures ranging from 25°C to 100°C. Thanks to this extraction, the A-Si: H TFT (Amorphous-Silicon: Hydrogenated Thin Film Transistors) model is modified to take into account the specific parameter dependences of the devices. The proposed model allows predicting correctly OTFTs' behavior with respect to the temperature and is used to design fully-printed organic PTAT voltage generators.

Keywords: Organic Thin Film Transistors, Parameter dependence, PTAT, Static modeling, A-Si:H TFT model, Temperature.

INTRODUCTION

Research on organic electronics has recently increased by far. This fact is due to the main advantages of organic polymers or small molecules which can be deposited using low cost manufacturing techniques in addition to their flexibility or their biodegradability. Despite the weak performance, the huge size or the process scattering compared with classic inorganic circuits, many logic [1]–[4] and analog organic circuits [5]–[7] have been tested and proved to be functional.

Concerning the organic devices modeling, it is made complex by some misunderstanding of the physical phenomena taking place in organic semiconductors, and very few papers dealing with OTFT modeling are based on a physics model [4], [6], [8], [9]. Recently, a compact model for OFETs (Organic Field Effect Transistors) based on the UMEM (Unified Model and Extraction Method) [10] have been proved to be functional with organic transistors in all operation regimes. Another work based on the use of a modified MOSFET model [11] also presented correct performances for top and bottom contact OTFT structures. However, in all the previous cited works, neither the temperature nor the scalability of the model are included and the model is only tested and validated with single-transistor characteristics.

The proposed model in this paper comes to cover these weaknesses in order to ease the organic device modeling. The A-Si: H TFT model initially planned for inorganic devices is chosen to model the device. This analytical model proved to be usable for organic OTFTs at fixed temperature and fixed geometry as reported in previous works [12]–[14]. Due to its incorporation in most commercial Computer Aided Design (CAD) tools, it allows the fast designing of complex circuits. However, regarding the temperature and geometry dependences, the model is not adapted to the designed OTFTs. So, the paper focalizes on merging the geometry and temperature dependences of extracted parameters using the iterative extraction method defined in [15].

This investigation leads to a single static model including geometry and temperature dependences in above threshold regime. This first model for organic transistors taking into account both geometry and temperature dependences can be used in commercial CAD tools like Cadence for example. It allows simulating a complete system in more realistic conditions. Indeed, the temperature dependence is a key point to design stable circuits in a variable environment. In this paper, PTAT voltage generators often used in sensors or reference circuits are simulated and measured in the paper. Correct performances despite a non-negligible scattering of the manufacturing process [16] are obtained.

The paper is divided into five parts. Section 2 quickly presents the A-Si: H TFT model parameters and previous works. Section 3 presents the method used to merge the parameter dependences found in previous works as well as the

proposed model. Section 4 shows the model performances and its validation. The final section is devoted to conclusions and presents future works.

DEVICE MODELING AND PREVIOUS WORKS

A. A-Si: H TFT model

1) Above-threshold regime parameters

For the above-threshold regime modeling, the parameters are extracted as in [17] added to our iterative method presented in [15]. The extracted parameters are mainly the power law mobility (γ), the threshold voltage (V_T), the band mobility (μ_0), the characteristic field voltage (V_{aa}), the series resistance (R), the saturation modulation parameter (α_{sat}), the channel length modulation (λ_{sat}) and the knee parameter (M).

2) Temperature parameters

The original A-Si: H TFT model already includes temperature dependence based on the field effect mobility energy activation ($E\mu$), the threshold voltage temperature parameter (K_{VT}) and the saturation temperature parameter ($K\alpha sat$) in above-threshold regime. This original dependence being not adapted to the designed OTFTs was thus suppressed and a new temperature modeling is proposed in the paper.

B. Previous works

In order to propose an adapted model to the OTFTs, the extraction procedure is performed at different temperatures on different geometries.

1) Temperature modeling

In a previous work [18], it has been showed that μ_0, γ and R parameters present a non-negligible temperature dependence at fixed geometry following (1), (2) and (3) where γ_T, $A\gamma_T$, μ_T, μ_{0T} R_T and A_{RT} are extraction-determined and T is the device temperature.

$$\gamma(T) = \gamma_T * T^{A_{\gamma T}} \tag{1}$$

$$\mu_0(T) = \mu_T * e^{(\mu_{0T} * T)} \tag{2}$$

$$R(T) = R_T * e^{(A_{RT} * T)} \tag{3}$$

2) Geometry scalability

At fixed temperature (ambient temperature ≈ 25°C), the empirical geometry dependences in [15] have been expressed following (4),(5), (6) and (7) where λ_L, $A_{\lambda L}$, α_L, $A_{\alpha L}$ μ_{WL}, $A_{\mu WL}$, R_{WL} and A_{RWL} are extraction-determined constants. W and L are respectively the width and the length of the OTFTs.

$$\lambda_{sat}(L) = \lambda_L * (L)^{A_{\lambda L}} \tag{4}$$

$$\alpha_{sat}(L) = \alpha_L * (L)^{A_{\alpha L}} \tag{5}$$

$$\mu_0\left(\frac{W}{L}\right) = \mu_{WL} * \left(\frac{W}{L}\right)^{A_{\mu WL}} \tag{6}$$

$$R\left(\frac{W}{L}\right) = R_{WL} * \left(\frac{W}{L}\right)^{A_{RWL}} \tag{7}$$

MERGING TEMPERATURE AND GEOMETRY DEPENDENCES INTO A SINGLE MODEL

In order to have one single model easing the design, the temperature and geometry dependences should be merged. To achieve this, the OTFTs with the highest band mobility (μ_0) and the highest series resistance (R) is set as reference, here the OTFTs having ratios of W/L=25. Then, the two parameters: R and μ_0, being both temperature- and geometry-dependent, are normalized in relation to the reference geometry. The obtained normalization coefficients do not vary significantly at different temperatures for each geometry as related in Table 1 for W/L=200 as example.

Tab le 1: Normalization coefficients of R and μ_0 for W/L=200 in relation to W/L=25 set as reference as function of the temperature.

Temperature (°C)	Normalization R coefficients, W/L=200	Normalization μ_0 coefficients, W/L=200
25	0.20	0.62
40	0.23	0.60
60	0.225	0.56
80	0.22	0.62
100	0.26	0.60

Based on these previous results, the band mobility and the series resistance merging geometry and temperature dependences can respectively be written following (8) and (9) where $\mu_{ref}(T)$ and $R_{ref}(T)$ are respectively the band mobility and series resistance temperature dependences of the chosen reference (W/L=25). $\mu_{norm}(W/L)$ and $R_{norm}(W/L)$ are respectively the normalization coefficients of extracted band mobility and series resistance for the different geometries as represented in Fig.1.

$$\mu_0\left(T,\frac{W}{L}\right)=\mu_{ref}(T)*\mu_{norm}\left(\frac{W}{L}\right) \tag{8}$$

$$R\left(T,\frac{W}{L}\right)=R_{ref}(T)*R_{norm}\left(\frac{W}{L}\right) \tag{9}$$

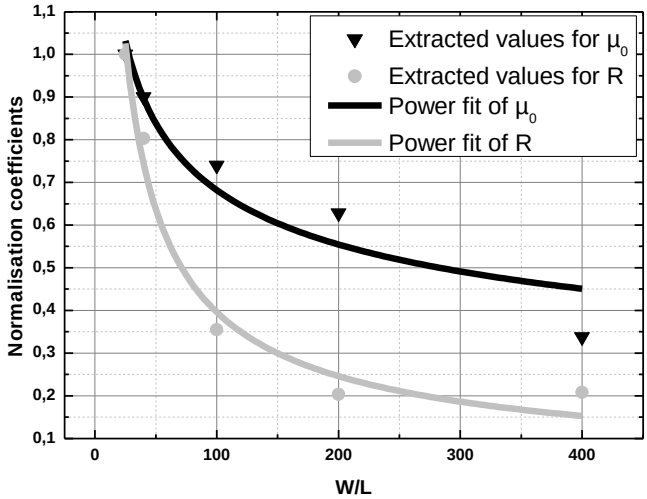

Fig. 1: Normalization coefficients of R and μ_0 in relation to W/L=25 set as reference, T=25°C

Therefore, the final proposed model merging geometry and temperature dependences can be written as in (10).

$$I_{ds}\left(T,L,\frac{W}{L}\right)=\frac{K*\mu_0\left(T,\frac{W}{L}\right)*\left[\frac{\left(V_{gs}-V_T\right)^{1+\gamma(T)}}{V_{aa}{}^{\gamma(T)}}\right]}{1+R\left(T,\frac{W}{L}\right)*K*\mu_0\left(T,\frac{W}{L}\right)*\left[\frac{\left(V_{gs}-V_T\right)^{1+\gamma(T)}}{V_{aa}{}^{\gamma(T)}}\right]}*V_{ds}*(1+\lambda_{sat}(L)*V_{ds})*\frac{1}{\left[1+\left(\frac{V_{ds}}{\alpha_{sat}(L)*(V_{gs}-V_T)}\right)^M\right]^{1/M}} \tag{10}$$

MODEL PERFORMANCE ANS VALIDATIONS

A. Model performance

To evaluate the model performance, as first step, modelled curves are compared with measurements for four different geometries at three different temperatures. From Fig.2 to Fig.4, the modelled and measured current derivatives (transconductance and output conductance) are compared. This comparison confirms a correct behavior of the proposed model regarding geometry and temperature variations even if there are some weaknesses in the saturation regimes of transconductance characteristics for W/L=40 and W/L=100 (Fig.2 and Fig.3). These weaknesses are mainly caused by the errors introduced when interpolating the empirical parameter dependences.

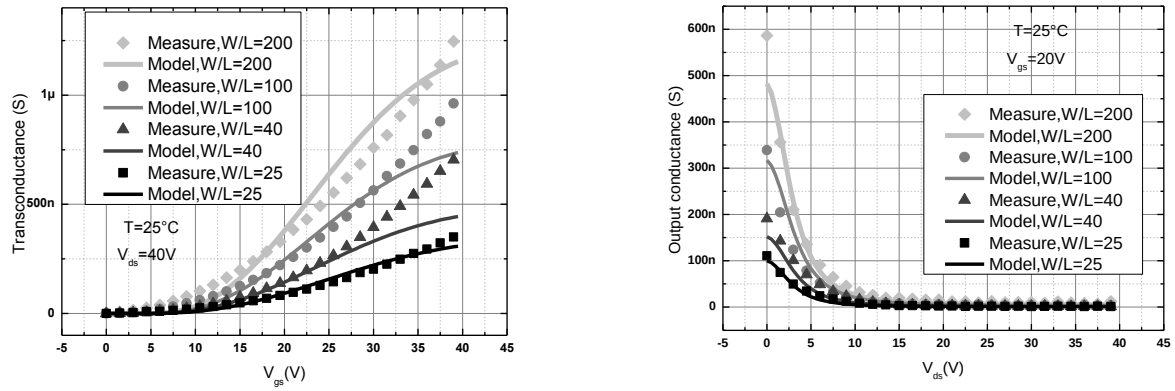

Fig. 2: Transconductances and output conductances for different geometries, T=25°C

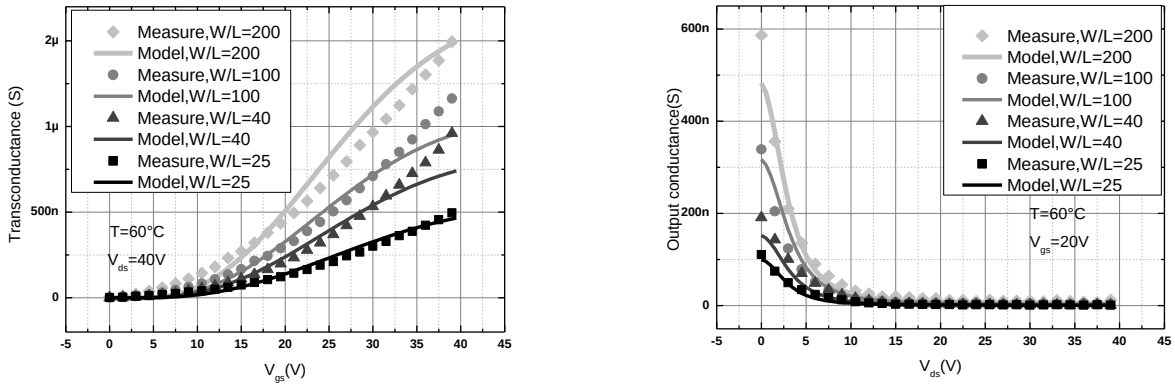

Fig. 3: Transconductances and output conductances for different geometries, T=60°C

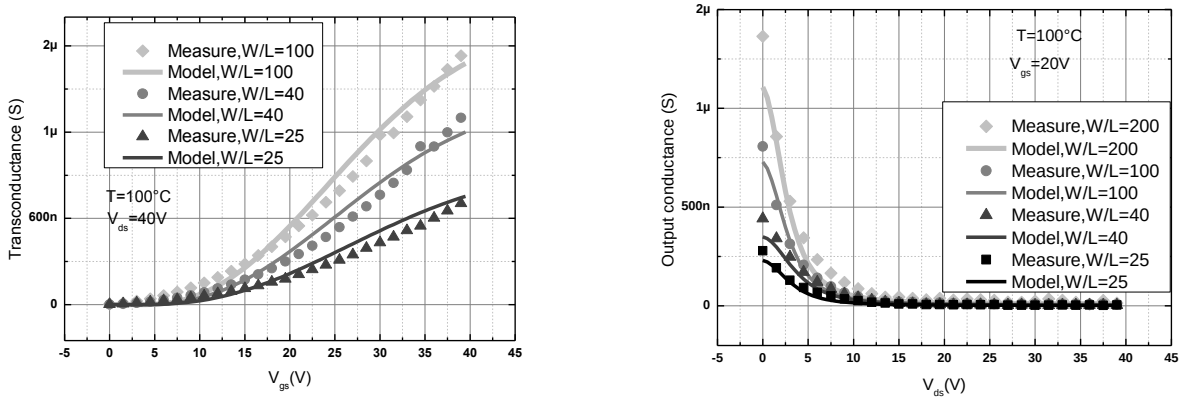

Fig. 4: Transconductances and output conductances for different geometries, T=100°C

B. Model validation

The following validation step is done by testing the model with designed organic PTAT voltage generators [19]–[21]. In Table 2, a benchmarking of the proposed model is presented. This table shows the effort done in temperature modeling compared with other works.

Table 2: Benchmarking of some works on static OTFTs modeling

	[10]	**[11]**	**[22]**	**[23]**	**This work**
Model	UMEM	Modified MOSFET	A-Si: H TFT	VRH	Modified A-Si: H TFT
Model card(s)	Several	Several	Several	Several	Single
Series resistance	YES	YES	NO	YES	YES
T° modeling	NO	NO	NO	NO	YES
Current derivatives validation	YES	-	NO	NO	YES
Dynamic modeling	NO	NO	NO	YES	NO
Validation with circuits	NO	YES	NO	YES	YES

1) PTAT circuit design

The designed organic PTAT voltage generators are based on the structure related in [20] by C. Rossi et al. In their work, they exploited the temperature dependence of the sub-threshold current in case of inorganic transistors. In this work, due to the non-negligible process dispersion of fully-printed technique as related in a previous work [16], the temperature dependence of the sub-threshold current is not obvious, then the fully-printed organic PTAT voltage generators are designed exploiting the temperature dependences in the above-threshold regime. Two types of PTAT voltage generators are presented in the paper, an N-PTAT with a 3-OTFTs current mirror and a P-PTAT with a 4-OTFTs current mirror. The electrical schematics and microscopic images of the two types are represented in Fig.5 and Fig.6.

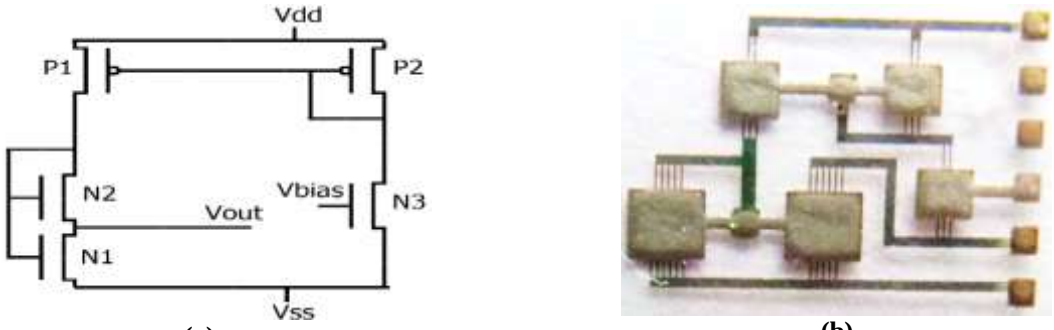

(a) **(b)**

Fig. 5: Schematic (a) and microscopic image (b) of a fully-printed N-type PTAT voltage generator

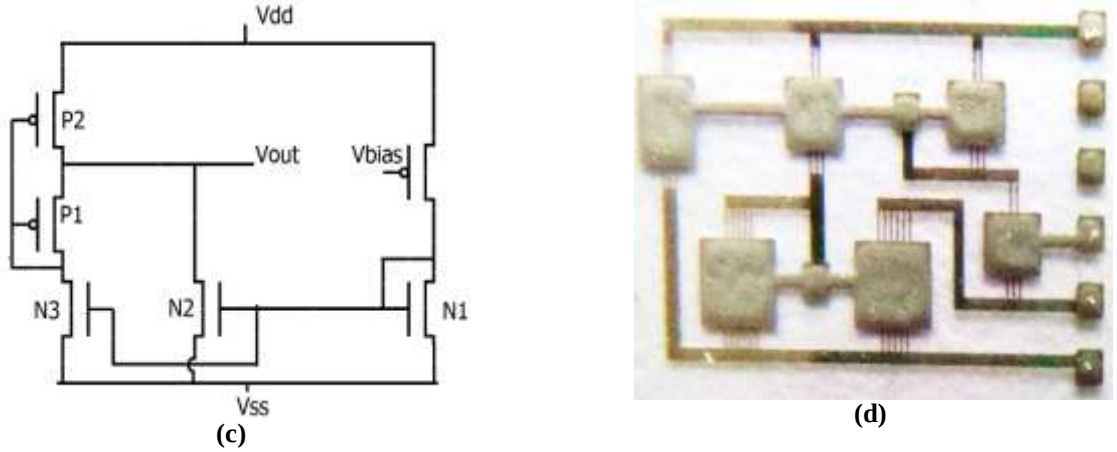

(c) **(d)**

Fig. 6: Schematic (c) and microscopic image (d) of a fully-printed P-type PTAT voltage generator

For the N-type, N1 and N2 OTFTs have both a size of W/L= 5000µm/20µm. N3 have a size of W/L=500µm/20µm, P1 and P2 had respectively sizes of W/L=1000µm/20µm and W/L=500µm/20µm. For the P-type, N1, N2 and N3 have respectively sizes of W/L=500µm/20µm, 1000µm/20µm and 2000µm/20µm. P1 and P2 have both size of W/L=5000µm/20µm.

2) PTAT Simulations and electrical characterization

The simulations are done using the proposed model in the paper tailored for N-Type. P-type modeling is also done using the same approach as for N-type but is not presented to avoid repetition. The circuits are characterized under +/-20V supply voltage at temperatures from 25°C to 80°C. The bias voltage is set at -20V for the N-type current mirror and at 20V for the P-type. In Fig.7, the modelled and measured output voltages as function of the temperature are represented. Despite a non-negligible process dispersion as related in [16], [24], the measured output as function of the temperature showed linear dependence with both positive slopes in simulations and measurements having respective values of 3,5mV/°C and 7,2mV/°C for N-type and 4mV/°C and 2,2 mV/°C for P-type. The N-type output is very close to Vss due the huge size of N-OTFTs compared with P-type. This disequilibrium is corrected in the P-type by considering a 4-OTFTs current mirror. Slight shifts of the measured outputs compared with simulations can be observed mainly due to the scattering of manufacturing process added to errors introduced when interpolating the empirical parameter dependences. However, the proposed model performance is quite correct with shifts lower than 1 V for P-type and lower than 2 V for N-type.

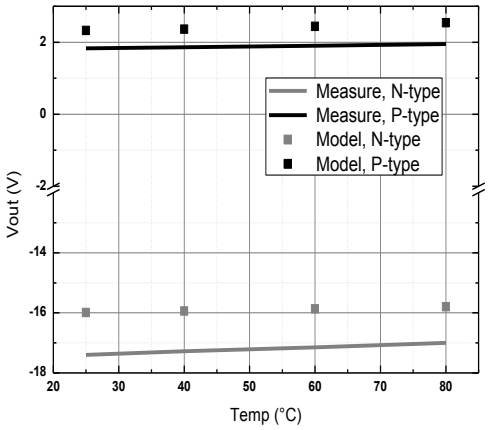

Fig. 7: Outputs of the designed fully-printed organic N- and P-type PTAT voltage generators as function of temperature

CONCLUSION

In this work, a complete static modeling in above-threshold regime for fully-printed OTFTs is done. The proposed model can be used to design rapidly complex organic circuits sensible to the temperature. Indeed, it is used to design organic PTAT voltage generators never related in organic electronics and correct performance are obtained. Future works will be to insert the dynamic model as done in [25], [26] and to propose a strong method of sub-threshold and leakage regimes modeling as done in [10], [27].

REFERENCES

[1]. M. Guerin, E. Bergeret, E. Benevent, A. Daami, P. Pannier, and R. Coppard, “Organic complementary logic circuits and volatile memories integrated on plastic foils,” IEEE Trans. Electron Devices, vol. 60, no. 6, pp. 2045–2051, 2013.

[2]. M. Guerin, E. Bergeret, E. Bènevent, P. Pannier, A. Daami, S. Jacob, I. Chartier, and R. Coppard, “Design of organic complementary circuits for RFID tags application,” Proc. Cust. Integr. Circuits Conf., 2012.

[3]. Abdinia, S.; Benwadih, M.; Coppard, R.; Jacob, S.; Maiellaro, G.; Palmisano, G.; Rizzo, M.; Scuderi, A.; Tramontana, F.; van Roermund, A.; Cantatore, E., "A 4b ADC manufactured in a fully-printed organic complementary technology including resistors," in Solid-State Circuits Conference Digest of Technical Papers (ISSCC), 2013 IEEE International , vol., no., pp.106-107, 17-21 Feb. 2013

[4]. B. Kumar, B. K. Kaushik, Y. S. Negi, and V. Goswami, “Single and dual gate OTFT based robust organic digital design,” Microelectron. Reliab., vol. 54, no. 1, pp. 100–109, 2014.

[5]. Abdinia, S.; Benwadih, M.; Cantatore, E.; Chartier, I.; Jacob, S.; Maddiona, L.; Maiellaro, G.; Mariucci, L.; Palmisano, G.; Rapisarda, M.; Tramontana, F.; van Roermund, A.H.M., "Design of analog and digital building blocks in a fully printed complementary organic technology," in ESSCIRC (ESSCIRC), 2012 Proceedings of the , vol., no., pp.145-148, 17-21 Sept. 2012.

[6]. S. Abdinia, F. Torricelli, G. Maiellaro, R. Coppard, A. Daami, S. Jacob, L. Mariucci, G. Palmisano, E. Ragonese, F. Tramontana, A. H. M. van Roermund, and E. Cantatore, “Variation-based design of an AM demodulator in a printed complementary organic technology,” Org. Electron., vol. 15, no. 4, pp. 904–912, Apr. 2014.

[7]. V. Fiore, E. Ragonese, S. Abdinia, S. Jacob, I. Chartier, R. Coppard, A. van Roermund, E. Cantatore, and G. Palmisano, “30.4 A 13.56MHz RFID tag with active envelope detection in an organic complementary TFT technology,” 2014 IEEE Int. Solid-State Circuits Conf. Dig. Tech. Pap., pp. 492–493, Feb. 2014.

[8]. N. P. Papadopoulos, A. Marsal, R. Picos, J. Puigdollers, and A. A. Hatzopoulos, “Simulation of organic inverter,” Solid. State. Electron., vol. 68, pp. 18–21, Feb. 2012.

[9]. A. Bonea, T. Hassinen, B. a. Ofrim, D. C. Bonfert, and P. Svasta, “Analytical modeling of contact resistance in organic transistors,” CAS 2012 (International Semicond. Conf., no. 1, pp. 399–402, Oct. 2012.

[10]. C. H. Kim, S. Member, A. Castro-carranza, M. Estrada, S. Member, A. Cerdeira, Y. Bonnassieux, G. Horowitz, and B. Iñiguez, “A Compact Model for Organic Field-Effect Transistors With Improved Output Asymptotic Behaviors,” in Electron Devices, IEEE Transactions on vol. 60, no. 3, pp. 1136–1141, 2013.

[11]. B. Kumar, B. K. Kaushik, Y. S. Negi, S. Saxena, and G. D. Varma, “Analytical modeling and parameter extraction of top and bottom contact structures of organic thin film transistors,” Microelectronics J., vol. 44, no. 9, pp. 736–743, Sep. 2013.

[12]. M. Estrada, A. Cerdeira, J. Puigdollers, L. Reséndiz, J. Pallares, L.F. Marsal, C. Voz, B. Iñiguez, Accurate modeling and parameter extraction method for organic TFTs, Solid-State Electronics, Volume 49, Issue 6, Pages 1009-1016, June 2005.

[13]. M. Estrada, I. Mejía, A. Cerdeira, J. Pallares, L. F. Marsal, and B. Iñiguez, “Mobility model for compact device modeling of OTFTs made with different materials,” Solid. State. Electron., vol. 52, no. 5, pp. 787–794, May 2008.

[14]. S. Jacob, A. Daami, R. Gwoziecki, and R. Coppard, “Fast behavioral modeling of organic CMOS devices for digital- and analog circuit applications,” Proc. SPIE 8117, Organic Field-Effect Transistors X, 81170Q ,September 07, 2011.

[15]. M. A. Sankhare, E. Bergeret, P. Pannier, and R. Coppard, “Static modeling of fully-printed OTFTs using a modified Amorphous-Si : H TFT model,” International Journal of Enhanced Research in Science, Technology & Engineering (IJERSTE), vol. 4, no. 7, pp. 1–10, October 2015.

[16]. Sankhare, M.A.; Bergeret, E.; Pannier, P.; Coppard, R., "Series resistances impacts on full-printed organic circuits," in Microelectronics (ICM), 2014 26th International Conference on , vol., no., pp.236-239, 14-17 Dec. 2014.
[17]. L. Reséndiz, M. Estrada, and a. Cerdeira, "New procedure for the extraction of a-Si:H TFTs model parameters in the subthreshold region," Solid. State. Electron., vol. 47, no. 8, pp. 1351–1358, Aug. 2003.
[18]. Sankhare, M.A.; Bergeret, E.; Pannier, P.; Coppard, R., "Temperature modeling of fully-printed OTFTs based on a modified A-Si: H TFT model," in Electron Devices and Solid-State Circuits (EDSSC), 2015 IEEE International Conference on , vol., no., pp.321-324, 1-4 June 2015.
[19]. C. Christoffersen, C.; Toombs, G.; Manzak, A., "An ultra-low power CMOS PTAT current source," in Argentine School of Micro-Nanoelectronics Technology and Applications (EAMTA), 2010 , vol., no., pp.35-40, 1-9 Oct. 2010.
[20]. C. Rossi, M. C. Schneider, and I. D. I. El, "PTAT Voltage Generator based on an MOS Voltage Divider," NSTI-Nanotech 2007, www.nsti.org, ISBN 1420061844 Vol. 3, 2007.
[21]. E. M. Camacho-Galeano, C. Galup-Montoro, and M. C. Schneider, "A 2-nW 1.1-V self-biased current reference in CMOS technology," IEEE Trans. Circuits Syst. II Express Briefs, vol. 52, no. 2, pp. 61–65, 2005.
[22]. Sankhare, M.A.; Bergeret, E.; Pannier, P.; Coppard, R., "Series resistances impacts on full-printed organic circuits," in Microelectronics (ICM), 2014 26th International Conference on , vol., no., pp.236-239, 14-17 Dec. 2014.
[23]. Zaki, T.; Scheinert, S.; Horselmann, I.; Rodel, R.; Letzkus, F.; Richter, H.; Zschieschang, U.; Klauk, H.; Burghartz, J.N., "Accurate Capacitance Modeling and Characterization of Organic Thin-Film Transistors," in Electron Devices, IEEE Transactions on , vol.61, no.1, pp.98-104, Jan. 2014.
[24]. O. Marinov and M. Jamal Deen, "Quasistatic compact modelling of organic thin-film transistors," Org. Electron., vol. 14, no. 1, pp. 295–311, Jan. 2013.
[25]. M. Estrada, "Extraction method for polycrystalline TFT above and below threshold model parameters," Solid State Electronics, Volume 46, Issue 12, p. 2295-2300, 2002.
[26]. O. Yaghmazadeh, Y. Bonnassieux, A. Saboundji, L. Cnrs-umr, E. Polytechnique, B. Geffroy, D. Tondelier, and G. Horowitz, Journal of the Korean Physical Society, "A SPICE-like DC Model for Organic Thin-Film Transistors," vol. 54, no. 1, pp. 523–526, 2009.
[27]. M. Fadlallah, G. Billiot, W. Eccleston, and D. Barclay, "DC/AC unified OTFT compact modeling and circuit design for RFID applications," Solid. State. Electron., vol. 51, no. 7, pp. 1047–1051, Jul. 2007.